Colloid Polym Sci 277:95–100 (1999)

SHORT COMMUNICATION

N. Hattori
H. Hirata
H. Okabayashi
M. Furusaka
C. J. O'Connor
R. Zana

Small-angle neutron-scattering study of bis(quaternaryammonium bromide) surfactant micelles in water. Effect of the long spacer chain on micellar structure

Received: 15 June 1998
Accepted: 22 July 1998

N. Hattori · H. Hirata
H. Okabayashi (✉)
Department of Applied Chemistry
Nagoya Institute of Technology
Gokiso-cho, Showa-ku,
Nagoya 466-8555, Japan

M. Furusaka
BSF
National Laboratory for High
Energy Physics, 1-1 Oho, Tsukuba-shi
Ibaraki 305-0801, Japan

C.J.O'Connor
Department of Chemistry
The University of Auckland
Private Bag 92019, Auckland
New Zealand

R. Zana
Institut C. Sadron, CNRS-ULP
6 rue Boussingault
F-67083 Strasbourg Cedex,
France

Abstract The microstructure of the normal micelles formed by dimeric surfactants with long spacers, $[Br^-(CH_3)_2N^+(C_mH_{2m+1})\text{-}(CH_2)_S\text{-}(C_mH_{2m+1})N^+(CH_3)_2Br^-$, $m = 10$ and $s = 8$, 10 and 12], has been investigated by small-angle neutron scattering and compared with previously reported results for micelles of the same dimeric surfactants with shorter spacers ($m = 10$ and $s = 2$, 3, 4 and 6). It was found that for dimeric surfactants with long spacers ($s = 8$ and 10), both micellar growth and variation in shape occur to only a small extent, if at all, compared with dimeric surfactants with short spacers. However, for the dimeric surfactant with the longest spacer, $s = 12$, the extent of micellar growth and shape variation is also large. These results are due to the differences in conformation of dimeric surfactants with short spacers ($s = 2$–6) compared with that of the surfactants with long spacers ($s = 8$–12).

Key words Long spacer – bis (quaternaryammonium bromide) – micelle – Small-angle-neutron scattering

Introduction

Bis(quaternaryammonium bromide) surfactants, also called dimeric surfactants (DS), of general formula

$$Br^-(CH_3)_2N^+(C_mH_{2m+1})\text{-}(CH_2)_s\text{-}(C_mH_{2m+1})N^+(CH_3)_2Br^-$$

in which two alkyldimethylammonium bromide moieties are connected by a polymethylene chain (referred to as spacer), continue to attract interest [1–9].

Alami et al. [5] have reported the solution behavior of DS. The differences in the values of their critical micelle concentrations (cmc) were interpreted in terms of the change in conformation of the surfactant and variation in the location of the spacer within the micelle. Furthermore, in order to gain more insight into the behavior of the spacer, they also investigated the behavior of a series of DS ($m = 12$, $s = 3$, 4, 6, 8, 10, 12, 14 and 16) at the air/water interface. By applying Gibb's Law to the surface-tension data, they found that the plot of the surface area per surfactant versus spacer-carbon number, s, went through a maximum for $s = 10$–12. This peculiar behavior was interpreted as reflecting a change in the location of the spacer from the water interface to the air side of the interface at $s \geq 10$.

Diamant and Andelman [6] presented a theoretical explanation for these results and pointed out that the conformational entropy of the spacer chain, as well as

the attractive and repulsive interactions of the surfactant molecules, is a predominant factor in the type of morphology of the aggregates at the interface.

In our previous paper [7], we reported results for the small-angle neutron-scattering (SANS) analysis of a series of DS with $m = 10$ and $s = 2$, 3, 4 and 6, and showed that the extent of micellar growth and the variation of micellar shape of these surfactants were strongly dependent upon the carbon number of the spacer.

The present study uses SANS spectra to determine the effect of long spacers on the aggregation number and shape of the micelles of DS with $m = 10$ and $s = 8$, 10 and 12.

Experimental

Materials

Bis(quaternaryammonium bromide) surfactants (DS: $m = 10$, $s = 8$, 10 and 12) were synthesized as described previously [3, 7]. Sample identity was confirmed by NMR and elemental analyses.

Conductivity measurements and cmc determination

The electrical conductivities of the sample solutions were measured with a conductivity meter CM 11P (TOA Electronics Ltd) at 25.0 ± 0.1°C. The plots of the specific electrical conductivity against surfactant concentration, C, were used to determine the cmc. The degree of ionization of the micelle, α, and the values of free-energy change per surfactant upon micellization, ΔG_0, were calculated by the method described previously [7]. The following results were obtained. For $m = 10$ and $s = 8$, cmc = 0.482 wt%, $\alpha = 0.32$ and $\Delta G_0 = -52.9$ kJmol^{-1}; for $m = 10$ and $s = 10$, cmc = 0.280 wt%, $\alpha = 0.37$ and $\Delta G_0 = -53.4$ kJmol^{-1}; for $m = 10$ and $s = 12$, cmc = 0.151 wt%, $\alpha = 0.39$ and $\Delta G_0 = -56.0$ kJmol^{-1}.

SANS measurements

The SANS measurements were carried out using the medium-angle neutron-scattering instrument (WINK) installed at the pulsed neutron source KENS at the National Laboratory for High Energy Physics, Tsukuba, Japan. The sample solutions were placed in a quartz cell of 1 or 2 mm path length at 23°C. The scattering length density (ρ) of each component was calculated using the equation

$$\rho = \Sigma b_i / V, \tag{1}$$

where b_i is the scattering length of atom i and V is the molecular volume. The V values and the values quoted from Refs. [7, 10, 11] were used. The magnitude of the momentum transfer, Q, is given by

$$Q = \frac{4\pi}{\lambda} \sin \frac{\theta}{2}, \tag{2}$$

where λ is the incident wavelength (1–16 Å for WINK). The intensity of the scattered neutrons was recorded on a position-sensitive 2D detector. Normalization of the data to an absolute intensity scale was made by using the transmission of a 1 mm water sample. Corrections for the attenuation of the neutron beam due to absorption and for multiple scattering were also made. In the SANS data analysis, the scattering intensity coming from the DS solution was corrected for the detector background and incoherent scattering. The intensity spectrum of the DS solution measured at concentrations below the cmc was subtracted from those of the micellar solutions in the Q range 0.06–0.30 Å^{-1}.

Analysis of SANS data

The dependence of the neutron-scattering intensity $d\Sigma(Q)/d\Omega$ on the magnitude of a scattering vector (Q) can be expressed as a function of both the micellar particle structure factor $P(Q)$ and the interparticle structure factor $S'(Q)$, as follows

$$d\Sigma(Q)/d\Omega = I_0 P(Q) S'(Q) \tag{3}$$

where I_0 is the extrapolated zero-angle scattering intensity, which is given in terms of the volumes of the

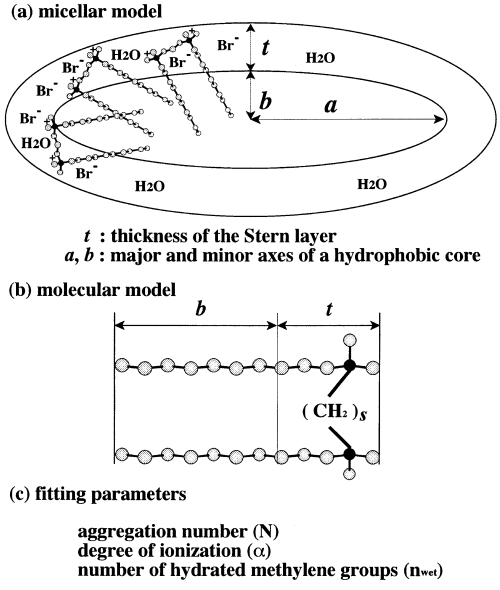

t : thickness of the Stern layer
a, b : major and minor axes of a hydrophobic core

Fig. 1a–c Micellar model used in the calculation of $P(Q)$ and the relationship between the molecular and fitting parameters

micellar core and the overall micelle and of the average neutron scattering length densities of the polar shell, hydrophobic core and solvent. The single micellar particle structure factor $P(Q)$ was calculated by application of the micellar model, as shown in Fig. 1. $S'(Q)$ is a function of the diameter, σ, the charge and number density of the micelles and of the dielectric constant of the solvent.

Hayter and Penfold [12] demonstrated that the SANS spectra coming from a micellar solution could be well-described by treating the solution as a one-component macrofluid. Furthermore, they provided a means of calculating an interparticle structure factor, $S'(Q)$, for a one-component macrofluid [12–14]. In this model, the micelle is assumed to be a rigid charged sphere of diameter σ [15, 16], interacting through a dimensionless screened Coulombic potential, which is calculated by using the inverse screening length of Debye-Hückel theory, defined by the ionic strength, I, of the solution. This assumption is reasonable for charged micelles if the a/b ratio is not much greater than unity. Furthermore, it has been shown that one may approximate the micellar core as a rigid sphere, provided that the shape of the ionic micelle is ellipsoidal with an a/b ratio no greater than 2[16].

Results and discussion

A structural model of the DS micelle has been proposed, based on the assumptions made in the analysis of the SANS spectra of *n*-alkyltrimethylammonium bromide micelles [11, 17, 18]. The shape of a DS micelle with $m = 10$ was thought to be prolate, with a hydrophobic core with a major axis, a, and minor axis, b. The b value was set equal to the fully extended length of the portion of the *n*-decyl chain which constitutes the hydrophobic core. The Stern layer, of thickness t, consists of the dimethylammonium head groups, associated with bromide counterions and water molecules, spacer methylene groups, and the hydrated portion of the *n*-decyl chain. In the present study, calculations were made for both prolate and oblate spheroidal models of the DS micelles. It was found that the prolate model consistently provided a better fit to the observed SANS intensity data than did the oblate model.

Figure 2 shows the SANS spectra of the DS micellar solutions at various concentrations. The observed scattering-intensity data were analyzed with the aggregation number, N, the degree of micellar ionization, α, and the number of hydrated methylene groups, n_{wet}, as fitting

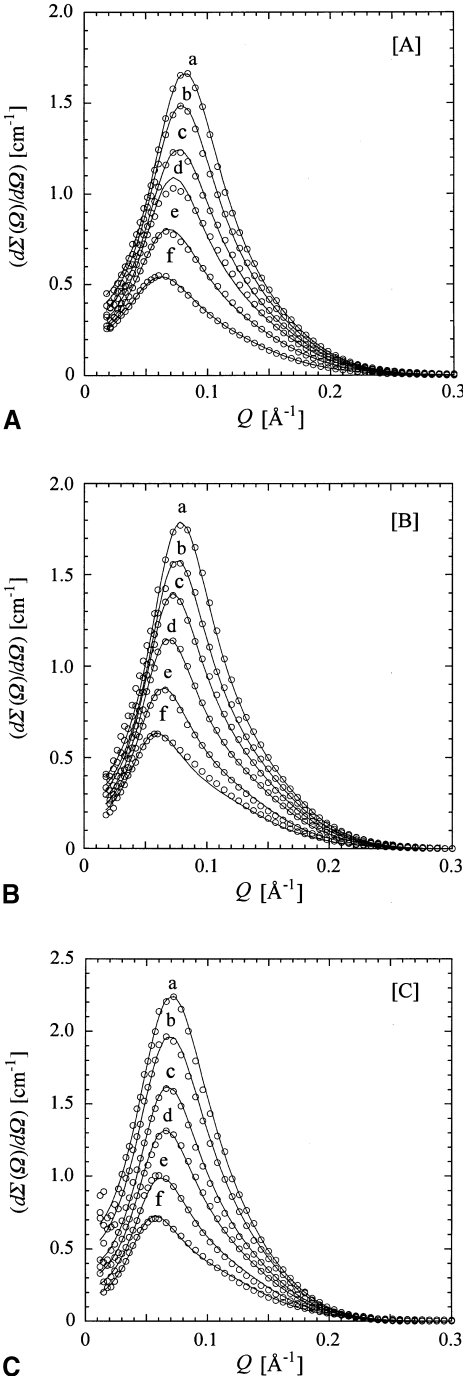

Fig. 2 A Observed scattering intensity spectra (*open circles*) for the dimeric surfactant (DS) ($m = 10$, $s = 8$)-D_2O system at 23°C. (*a*) 4.0 wt%, (*b*) 3.5 wt%, (*c*) 3.0 wt%, (*d*) 2.5 wt%, (*e*) 2.0 wt%, (*f*) 1.5 wt% and (*g*) 1.0 wt%, and theoretically calculated spectra (*solid lines*). Average deviation per datum point is within ±3.0% for all spectra. **B** Observed scattering intensity spectra (*open circles*) for the DS ($m = 10$, $s = 10$)-D_2O system at 23°C. (*a*) 4.0 wt%, (*b*) 3.5 wt%, (*c*) 3.0 wt%, (*d*) 2.5 wt%, (*e*) 2.0 wt%, (*f*) 1.5 wt% and (*g*) 1.0 wt%, and theoretically calculated spectra (*solid lines*). Average deviation per datum point is within ±6.1% for all spectra. **C** Observed scattering intensity spectra (*open circles*) for the DS ($m = 10$, $s = 12$)-D_2O system at 23°C. (*a*) 4.0 wt%, (*b*) 3.5 wt%, (*c*) 3.0 wt%, (*d*) 2.5 wt%, (*e*) 2.0 wt%, (*f*) 1.5 wt% and (*g*) 1.0 wt%, and theoretically calculated spectra (*solid lines*). Average deviation per datum point is within ±3.8% for all spectra

parameters, and the values of a, b and t were calculated using n_{wet} and N. The intensity spectra were calculated by assuming monodispersity for these micellar solutions. Very broad peaks are observed in the curves of $I(Q)$ against Q, showing that there are interactions between the micelles. Moreover, as the concentration increases the peak increases steadily in intensity and shifts to higher Q values, indicating enhanced interparticle interactions with increasing micellar concentration. The values of the extracted parameters are listed in Table 1. The closeness of fit between the observed and theoretically calculated data is excellent. The average percentage deviation per datum point is within ± 2–4% for all spectra.

It can be seen from the data in Table 1 that the ratio of $(a+t)/(b+t)$ for the prolate spherical micelle changes little within the range 1.0–1.1 for the DS with $s = 8$ and 10, but that is gradually increases within the range 1.0–1.25 for the DS with $s = 12$. Therefore, we may assume that at $s = 8$ and 10 no variation in shape (from sphere to prolate) occurs upon increasing micellar concentration, while at $s = 12$, a variation in shape occurs, although only to a small extent.

Extrapolation of the linear plot of aggregation number N vs. $(X - X_{cmc})^{1/2}$ (X and X_{cmc} are the surfactant concentration and cmc expressed as molar fractions) gives the minimum aggregation number, N_0, of the micelles at the cmc (Fig. 3). The values of N_0 are listed in Table 2. For the DS with $s = 8$ and 10, the N_0 values are the same within experimental error (17–18, respectively), while for the DS with $s = 12$ the N_0 value is smaller (13). Since the N_0 values for the DS with short spacers ($s = 2$–6) are ($N_0 = 22$–25 [7], it is clear that there is a difference in the N_0 values of the DS with long and short spacers. This observation may reflect a progressive penetration of the spacer into the micellar core at $s \geq 8$.

In a previous paper [7], we reported a SANS study on the effect of the spacer length in DS with shorter spacers ($m = 10$ and $s = 2$, 3, 4 and 6) on the micellar growth and variation in shape (from sphere to prolate) of their micelles in water. The results may be summarized as follows. A ladder model of micellar growth could be applied to the micelle formation by DS. The slope in the linear plots of N versus $(X - X_{cmc})^{1/2}$ decreased with an increase in spacer length (Fig. 3), indicating that the

Table 1 Experimental scattering intensity spectra of dimeric surfactant (DS) micellar solutions and theoretically calculated parameters

wt%	N	α	n_{wet}	a [Å]	b [Å]	t [Å]	$(a+t)(b+t)$	N_s	$1/\kappa$ [Å]	σ [Å]
DS ($m = 10$, $s = 8$)-D_2O systems at 23 °C										
1.5	18.9	0.39	3.2	11.6	13.8	9.5	1.10	45.1	19.3	43.7
2.0	19.1	0.41	2.6	12.3	13.4	8.4	1.05	40.5	18.2	43.0
2.5	19.8	0.42	2.6	12.4	13.8	8.8	1.07	39.0	17.2	43.2
3.0	19.9	0.36	2.7	12.2	14.0	8.9	1.08	39.6	17.0	43.5
3.5	20.6	0.34	2.8	12.1	14.6	9.1	1.12	39.6	16.6	44.0
4.0	20.7	0.31	3.0	11.8	15.0	9.4	1.15	41.0	16.3	44.4
DS ($m = 10$, $s = 10$)-D_2O systems at 23 °C										
1.5	19.1	0.47	2.3	12.8	13.0	8.4	1.01	36.1	22.0	42.4
2.0	19.3	0.43	3.1	11.7	14.0	9.4	1.11	42.1	21.0	43.8
2.5	19.7	0.43	2.3	12.8	13.4	8.4	1.03	35.3	19.7	42.7
3.0	20.1	0.39	2.5	12.5	13.9	8.7	1.07	36.2	19.2	43.2
3.5	20.0	0.31	2.6	12.3	14.0	8.8	1.08	36.9	19.3	43.3
4.0	20.3	0.29	2.6	12.4	14.2	8.8	1.08	36.3	19.1	43.5
DS ($m = 10$, $s = 12$)-D_2O systems at 23 °C										
1.5	21.1	0.44	1.6	13.6	13.6	7.5	1.00	26.8	24.3	42.3
2.0	21.6	0.36	2.2	12.9	14.5	8.2	1.08	30.1	23.6	43.4
2.5	22.9	0.31	2.2	12.9	15.5	8.3	1.12	28.6	23.0	44.0
3.0	24.1	0.27	2.5	12.5	16.6	8.6	1.19	29.3	22.6	45.0
3.5	25.6	0.22	2.2	12.9	17.2	8.2	1.20	25.9	22.8	45.1
4.0	26.4	0.20	2.3	12.7	18.0	8.4	1.25	26.2	22.7	45.8

(N average micellar aggregation number, α degree of ionization of the micelle, n_{wet} number of hydrated methylene groups in the Stern layer, a major axis of a prolate micelle given by $a = (4\pi N V_{tail})/(3b^2)$, b minor axis of a prolate micelle given by $b = 2.95 + 1.27(10 - n_{wet})$, t thickness of the Stern layer given by $t = 2.95 + 1.27(2 + n_{wet})$, N_s number of water molecules associated with a DS molecule, $1/\kappa$ inverse Debye-Huckel screening length, σ macroion diameter.)

Table 2 Minimum aggregation number (N_0) obtained from the linear plots of N vs $(X - X_{cmc})^{1/2}$

s	2	3	4	6	8	10	12
N_0	25	23	24	22	17	18	13

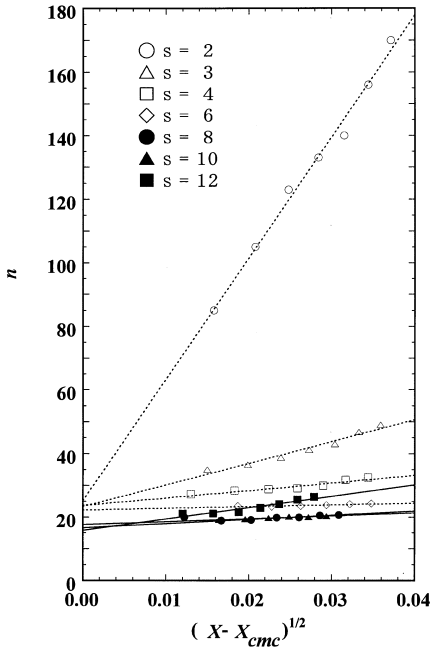

Fig. 3 Variation of n with $(X - X_{\mathrm{cmc}})^{1/2}$ for the DS ($m = 10$, $s = 8$, 10, 12). The plots for DS with $m = 10$ and $s = 2$, 3, 4 and 6 are from Ref.[7]

extent of micellar growth decreased as the spacer lengthened. In particular, it should be noted that there was a marked difference in the slopes for the two DS with $s = 2$ and 3 and that marked growth in the micelle occurred for the former DS. However, for the DS with $s = 6$, the slope of the linear plot approached zero, indicating that the extent of micellar growth was either very small or nonexistent.

We may now compare the results of the SANS analysis for a series of DS with longer spacers ($s = 8$, 10 and 12) with those for the DS with shorter spacers ($m = 10$ and $s = 2$, 3, 4 and 6). As seen in Fig. 3, the slopes for the DS with $s = 8$ and 10 are the smallest in the series. Therefore, it may be assumed that for the DS with $s = 8$ and 10 the extent of micellar growth becomes very small and that minimal micellar growth occurs. It should be noted that the slope for the DS with $s = 12$ again becomes larger, indicating an onset of micellar growth at this spacer length.

A ladder model for the process of micellization may be assumed [19], as follows. At the cmc, DS molecules form spherical micelles, of minimum size, which contain N_0 surfactants in aqueous solution and formation of micelles with an aggregation number less than N_0 does not occur. When DS micelles with $N > N_0$ are formed in solution, the micelle takes up the shape of a prolate spherocylinder and N_0 and $(N - N_0)$ molecules are used for formation of the hemispherical end portions and the cylindrical portion of the micelle, respectively. Therefore, the formation and growth of the micelles are characterized by the aggregation number, N_0, of the micelle of minimum size, the free-energy change, δ, per surfactant when a surfactant is inserted into the cylindrical portion of a spherocylindrical micelle, and the free-energy change, Δ, when N_0 surfactants aggregate to form this minimum micelle. The mean aggregation number, N, of a spherocylindrical micelle can be approximately given by

$$N = N_0 + 2K^{1/2}(X - X_{\mathrm{cmc}})^{1/2} \quad , \tag{4}$$

where $K = \exp[(\Delta - N_0\delta)/RT$. Therefore, the slope of the linear plots N vs. $(X - X_{\mathrm{cmc}})^{1/2}$ is equal to $2K^{1/2}$. The magnitude of $(\Delta - N_0\delta)$, calculated from the slope, represents the difference in free energy between N_0 surfactants in the two end caps of a spherocylindrical micelle and the same number of surfactants in the cylindrical portion. The value of $-(\Delta - N_0\delta)$ provides a measure of the rate of micellar growth as the concentration increases.

The calculated energy differences for DS with $s = 8$, 10 and 12 thus obtained are plotted against the spacer-carbon number (Fig. 4) together with the values for the series of DS with $s = 2$–6. As the spacer-carbon number increases, the parameter $-(\Delta - N_0\delta)$ increases exponentially for s in the range of $s = 2 - 8$, reaches its maximum between $s = 8$ and 10, then starts to decrease at $s = 12$. This variation in the energy difference indicates that increasing spacer-carbon number when $s < 10$ prevents micellar growth, but that when $s = 10$ the micelle starts to grow again. The observation that the parameter $-(\Delta - N_0\delta)$ goes through a maximum is very similar to the appearance of a maximum in a plot of surface area per surfactant vs. spacer-carbon number, reported by Alami et al. [5].

For a series of DS with $m = 12$, and $s = 3$, 4, 6, 8, 10, 12, 14 and 16, Alami et al. [5] postulated that when these

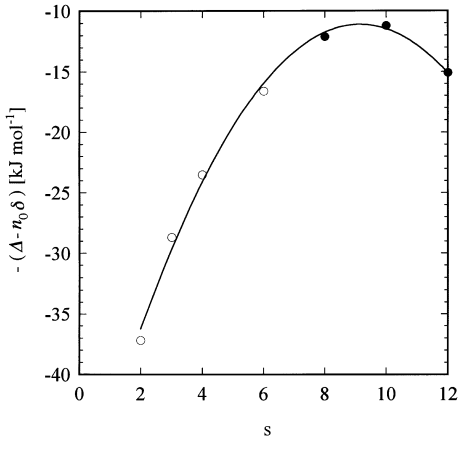

Fig. 4 Spacer chain-length dependence of $-(\Delta - N_0\delta)$ on the spacer-carbon number, s. The *open circles* are the data for the DS with $m = 10$ and $s = 2$, 3, 4 and 6 (from Ref.[7]). The *filled circles* are the data for DS with $m = 10$ and $s = 8$, 10 and 12

DS molecules were adsorbed at the air/water interface, those with $s < 10$ allowed the spacer to be in contact with the water, but lying more or less extended at the air/water interface, while for those with $s = 10$–12 the spacer adopted a folded conformation. That is, the surface tension data at the air/water interface suggested a conformational change of the spacer which was induced by an increase in its chain length. Direct spectroscopic evidence for such a conformational change has not yet been obtained. However, we suggest that this concept may be applied to the case of the aqueous micelles formed by the DS molecules in this investigation.

Diamant and Andelman [6] found that the dependency of the specific area of dimers at an air/water interface on the nature of the spacer is dominated by the interplay of three factors: the first is the geometrical effect of lengthening the spacer, which increases the specific area; the second is the interaction among the surfactant monomers, which decreases the specific area; and the third is the conformational entropy of the spacer chain, which enhances the effect of the second factor.

In general, as the number of carbon atoms in *n*-paraffins decreases, the probability of the *n*-paraffins taking up an all-*trans* conformation increases. Raman spectra of *n*-paraffins support this assumption. Indeed, the longitudinal accordion modes characteristic of extended polymethylene chains in a solid were found to remain very strong in the liquid state for the low homologs of *n*-paraffins (from *n*-butane to *n*-dodecane), while the accordion band at 150 cm^{-1} for solid cetane disappeared in the liquid state [20]. This means that for the shorter homologs the extended molecular form is abundant in the liquid state, while for cetane it is almost absent.

Furthermore, Okabayashi and coworkers [21] have demonstrated in Raman scattering studies of surfactant-water binary systems that a conformational change of surfactant molecules occurs upon micellization and that a specific rotational isomer (in particular, an all-*trans* form) is preferentially stabilized. It is evident that preferential stabilization of the all-*trans* form brings about variation in the packing parameters, affecting such morphology as micellar size and shape. Such preferential stabilization of the all-*trans* form may promote the first of the three factors proposed by Diamant and Andelman [6].

For the DS samples, with $s = 2$–12, we may expect that preferential stabilization of the all-*trans* form occurs upon micellization for $s \leq 10$ and that the populations of the conformers containing a *gauche* form become predominant with an increase in spacer-carbon number to $s > 10$. This trend may cause the appearance of a maximum in the plots of the calculated energy differences versus s.

Recently, for the DS molecule with $m = 10$ and $s = 6$, we have observed longitudinal accordion-like vibrational bands at 198–205 cm^{-1} in the solid state and in micellar solution (data not shown). Since the accordion vibrational modes of a hydrocarbon chain are characteristic of its extended form, this observation shows that the population of the all-*trans* form for the spacer with $s = 6$ is high in aqueous solution and that this isomer is preferentially stabilized in micellar solution. The Raman scattering spectra of DS molecules with $m = 10$ and $s = 8$, 10 and 12 and of the spacer-related compounds with similar spacers is under investigation, and these are expected to support the SANS results reported above.

References

1. Devinsky F, Lacko I, Imam T (1991) J Colloid Interface Sci 143:336–342
2. Zana R, Benrraou M, Rueff R (1991) Langmuir 7:1072–1075
3. Alami E, Levy H, Zana R, Skoulios A (1993) Langmuir 9:940–944
4. Zana R, Talmon Y (1993) Nature 362:228–230
5. Alami E, Beinert G, Marie P, Zana R (1993) Langmuir 9:1465–1467
6. Diamant H, Andelman D (1994) Langmuir 10:2910–2916
7. Hirata H, Hattori N, Ishida M, Okabayashi H, Furusaka M, Zana R (1995) J Phys Chem 99:17778–17784
8. Zhu Y-P, Masuyama A, Kirito Y, Okahara M, Rosen MJ (1992) J Am Oil Chem Soc 69:626–632 and references cited therein
9. Song LD, Rosen MJ (1996) Langmuir 12:1149–1153
10. Etori H, Hirata H, Yamada Y, Okabayashi H, Furusaka M (1997) Colloid Polym Sci 275:263–273
11. Berr SS, Caponetti E, Johnson JS Jr, Jones RRM, Magid LJ, (1986) J Phys Chem 90:5766–5770
12. Hayter JB, Penford J (1981) J Chem Soc Faraday Trans 1, 77:1851–1863
13. Hayter JB, Penford J (1981) Mol Phys 42:109–118
14. Hansen J, Hayter JB (1982) Mol Phys 46:651–656
15. Kotlarchyk M, Chen SH (1983) J Chem Phys 79:2461–2469
16. Chen SH, Lin TL (1987) Methods of experimental physics, vol 23, part B. Academic, London, pp 489–543
17. Berr SS, Coleman MJ, Jones RRM, Johnson JS Jr (1986) J Phys Chem 90:6492–6499
18. Berr SS (1987) J Phys Chem 91:4760–4765
19. Missel PJ, Mazer NA, Benedek GB, Young CY, Carey MC (1980) J Phys Chem 84:1044–1057
20. Mizushima S, Simanouti T (1949) J Am Chem Soc 71:1320–1324
21. (a) Okabayashi H, Okuyama M, Kitagawa T (1975) Bull Chem Soc Jpn 48:2264–2269; (b) Okabayashi H, Abe M (1980) J Phys Chem 84:999–1005; (c) Okabayashi H, Yoshida T, Ikeda T, Matsuura H, Kitagawa T (1982) J Am Chem Soc 104:5399–5402; (d) Okabayashi H, Taga K, Tsukamoto K, Tamaoki H, Yoshida T, Matsuura H (1985) Chem Scr 25:153–156; (e) Tsukamoto K, Ohshima K, Taga K, Okabayashi H, Matsuura H (1987) J Chem Soc Faraday Trans 1 83:789–800; (f) Okabayashi H, Tsukamoto K, Ohshima K, Taga K, Nishio E (1988) J Chem Soc Faraday Trans 1 84:1639–1651